

## **Supplemental information**

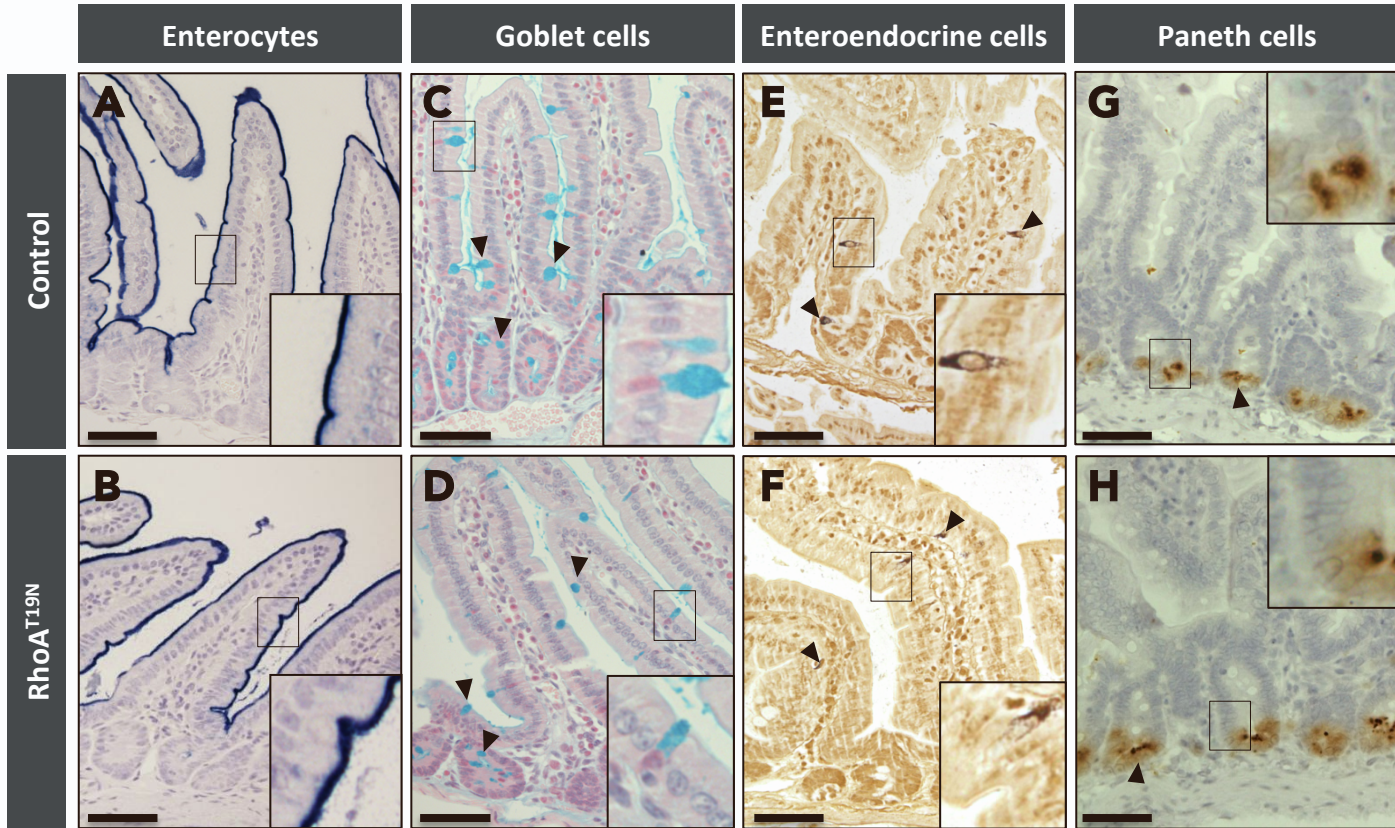
**RhoA downregulation in the murine**

**intestinal epithelium results in chronic**

**Wnt activation and increased tumorigenesis**

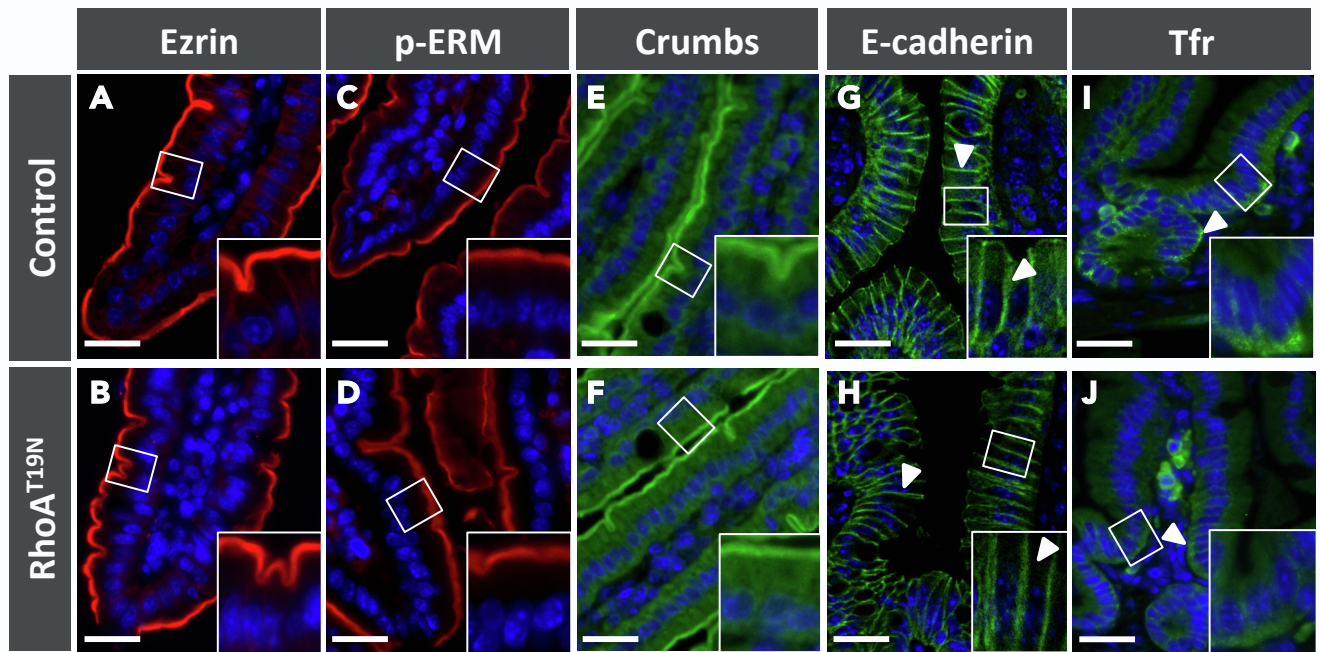
**Higinio Dopeso, Paulo Rodrigues, Fernando Cartón-García, Irati Macaya, Josipa Bilic, Estefanía Anguita, Li Jing, Bruno Brotons, Núria Vivancos, Laia Beà, Manuel Sánchez-Martín, Stefania Landolfi, Javier Hernandez-Losa, Santiago Ramon y Cajal, Rocío Nieto, María Vicario, Ricard Farre, Simo Schwartz Jr., Sven C.D. van Ijzendoorn, Kazuto Kobayashi, Águeda Martínez-Barriocanal, and Diego Arango**

# Supplementary Figure 1



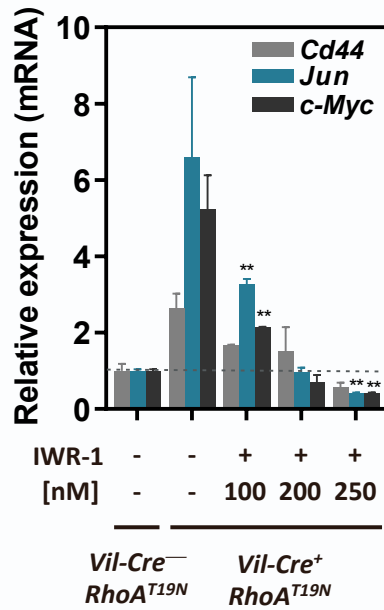
**Supplementary Figure 1: Effects of RhoA inhibition on intestinal epithelial cell lineage fate, related to Figure 5.** The number of total (A-B), goblet (C-D), enteroendocrine (E-F) and Paneth (G-H) cells were quantified in both villus and crypt compartments of the small intestine of control (*Vil-Cre*<sup>-</sup>;*RhoA*<sup>T19N</sup>) and *RhoA*<sup>T19N</sup> (*Vil-Cre*<sup>+</sup>;*RhoA*<sup>T19N</sup>) mice. Total cells were detected by hematoxylin counterstaining in alkaline phosphatase stained preparations (differentiated enterocytes; A-B), goblet cells were detected with alcian blue staining (C-D), enteroendocrine cells were detected with Grimelius staining (E-F) and Paneth cells were immunostained with an anti-lysozyme antibody (G-H). Arrows heads indicate examples of the different epithelial cell types. Scale bar: 50  $\mu$ m.

## Supplementary Figure 2



**Supplementary Figure 2: Localization of apical and basolateral protein markers in the intestinal cells of control and RhoA<sup>T19N</sup> mice, related to Figure 5.** Immunofluorescence staining of Ezrin (A-B) p-ERM (C-D), Crumbs (E-F), E-cadherin (G-H), and transferrin receptor (TfR) (I-J) in sections of the small intestine of control (*Vil-Cre<sup>-</sup>;RhoA<sup>T19N</sup>*) and RhoA<sup>T19N</sup> (*Vil-Cre<sup>+</sup>;RhoA<sup>T19N</sup>*) mice. Scale bar: 25  $\mu$ m.

## Supplementary Figure 3



### Supplementary Figure 3: Effects of the inhibition of RhoA<sup>T19N</sup>-dependent Wnt activation, related to Figure 8.

Relative levels of expression of the Wnt target genes *Cd44*, *Jun* and *c-Myc* in small intestinal organoids derived from *RhoA<sup>T19N</sup>* (*Vil-Cre<sup>+/+</sup>;RhoA<sup>T19N</sup>*) and control (*Vil-Cre<sup>-/-</sup>;RhoA<sup>T19N</sup>*) mice after treatment with increasing concentrations of the Wnt inhibitor IWR-1-endo. The mean  $\pm$ SEM in three independent experiments each of them carried out in triplicate is shown. Student's t-test \* $p < 0.05$ ; \*\* $p < 0.01$  (IWR1-treated *Vil-Cre<sup>+/+</sup>;RhoA<sup>T19N</sup>* vs *Vil-Cre<sup>-/-</sup>;RhoA<sup>T19N</sup>*).